

RESEARCH

Decreased sirtuin 4 levels promote cellular proliferation and invasion in papillary thyroid carcinoma

Hyun-Jin Lee^{1,2}, Young-Sool Hah³, So Young Cheon³, Seong Jun Won^{1,4,5}, Chae Dong Yim^{1,4,5},
Somi Ryu^{1,4,5}, Seung-Jun Lee⁶, Ji Hyun Seo^{5,7} and Jung Je Park^{1,3,4,5}

¹Department of Otorhinolaryngology-Head and Neck Surgery, Gyeongsang National University College of Medicine, Jinju, South Korea

²Department of Otorhinolaryngology-Head and Neck Surgery, Chung-Ang University College of Medicine, Seoul, South Korea

³Biomedical Research Institute, Gyeongsang National University Hospital, Jinju, South Korea

⁴Department of Otorhinolaryngology-Head and Neck Surgery, Gyeongsang National University Hospital, Jinju, South Korea

⁵Institute of Health Sciences, Gyeongsang National University, Jinju, South Korea

⁶Department of Convergence of Medical Sciences, Gyeongsang National University, Jinju, South Korea

⁷Department of Pediatrics, Gyeongsang National University College of Medicine, Jinju, South Korea

Correspondence should be addressed to JJ Park: capetown@hanmail.net

Abstract

Objective: This study examined the effect of sirtuin 4 (SIRT4), a NAD⁺-dependent deacetylase, on the proliferation and progression of papillary thyroid carcinoma (PTC).

Methods: Data from The Cancer Genome Atlas (TCGA) were analyzed to identify SIRT4 expression in thyroid cancer. Subsequently, the correlation between SIRT4 expression and clinical characteristics was examined in 205 PTC tissue samples. *In vitro* assays using three human thyroid cancer cell lines (B-CPAP, TPC-1, and SNU-790) were conducted to assess the effects of regulated SIRT4 expression on cell growth, apoptosis, invasion, and migration. Furthermore, *in vivo* experiments were performed in a xenograft mouse model.

Results: Gene Expression Omnibus (GEO) and TCGA data indicated that *SIRT4* expression is lower in thyroid cancer and *SIRT4* downregulation is associated with poor overall survival. In PTC tissues, positive SIRT4 expression was associated with decreased extracapsular extension. In *in vitro* experiments using three human thyroid cancer cell lines, overexpression of *SIRT4* decreased cell survival, clonogenic potential, and invasion and migratory capabilities, as well as inducing apoptosis and increasing reactive oxygen species levels. SIRT4 overexpression upregulated E-cadherin and downregulated N-cadherin, suggesting its potential involvement in the regulation of epithelial–mesenchymal transition. These findings were confirmed *in vivo* using a xenograft mouse model.

Conclusion: This study provides novel insight into the potential contribution of SIRT4 to the regulation of the pathological progression of PTC. The data suggest that SIRT4 plays a tumor-suppressive role in PTC by inhibiting growth, survival, and invasive potential. Future research should investigate the molecular mechanisms underlying these effects of SIRT4.

Keywords: epithelial–mesenchymal transition; papillary thyroid cancer; reactive oxygen species; SIRT4 protein; thyroid cancer

Introduction

Papillary thyroid carcinoma (PTC) is the most common subtype of thyroid cancer, accounting for more than 90% of all thyroid cancers (1). PTC is generally an indolent tumor with a relatively favorable prognosis; indeed, the 10-year survival rate is approximately 93% (2). Most cases are treated effectively by surgical resection followed by radioactive iodine therapy; however, in some cases, the disease shows an aggressive nature and does not respond to conventional treatments. Approximately 10% of patients experience recurrence, which is frequently associated with distant metastasis (3). Factors related to the prognosis and recurrence of PTC include age, stage, lymph node metastasis, extrathyroid extension, angioinvasion, and distant metastasis (4, 5). Moreover, reactive oxygen species (ROS) play a significant role in suppressing the progression of thyroid cancer (6, 7), whereas factors related to glutamine metabolism are involved in thyroid cancer tumorigenesis (8, 9). Nevertheless, the precise factors contributing to the progression of PTC remain unclear. Therefore, increasing our understanding of the molecular mechanisms underlying the proliferation and progression of PTC is important.

Sirtuins are a family of nicotinamide adenine dinucleotide (NAD⁺)-dependent deacetylases that are involved in numerous cellular processes, such as energy metabolism, chromosomal stability, DNA repair, cell cycle progression, and apoptosis (10). Seven sirtuin isoforms (SIRT1 to SIRT7) have been identified in mammals, each with a distinct subcellular localization and target proteins. SIRT4, a member of the Sirtuin family, is primarily located in mitochondria. It is associated with various biological processes, including glucose and lipid metabolism, mitochondrial function, and oxidative stress responses (11). A possible link between SIRT4 and cancer progression was recently proposed (12, 13, 14, 15, 16). SIRT4 has been characterized as a tumor suppressor, and SIRT4 is downregulated in several malignancies including thyroid cancer (14, 15). However, the precise function of SIRT4 in cancer remains unclear, and its involvement in cancer development has been suggested (12, 16).

There are a few studies focusing on SIRT4 in thyroid cancer, and its role in this malignancy has not been well characterized despite the association between SIRT4 and different types of cancer. In this study, we used a stepwise approach to examine the expression and biological function of SIRT4 in thyroid cancer, particularly PTC. First, we analyzed data from the Gene Expression Omnibus (GEO) and The Cancer Genome Atlas (TCGA) database, along with corresponding clinical data on the *SIRT4* in thyroid cancer. Next, we examined SIRT4 expression in PTC tissues and its association with clinical characteristics. *In vitro* analysis of thyroid cancer cell lines and *in vivo* studies using a xenograft

mouse model were performed to determine the effects of SIRT4 expression on cell growth, apoptosis, invasion, and migration and to identify the factors contributing to the effects of SIRT4 on thyroid cancer.

Materials and methods

Patient samples and data collection

The study was approved by the Institutional Review Board of Gyeongsang National University (GNUH 2023-07-027). All procedures were performed in accordance with the 1975 Declaration of Helsinki. In total, 205 tissue samples were obtained from patients diagnosed with PTC who underwent surgery at our hospital between 2011 and 2018. The patients' medical records were retrospectively reviewed, and clinical and pathological parameters were recorded. Immunohistochemical (IHC) studies were performed on all 205 tissues, and tissue microarrays were incubated overnight at 4°C with anti-SIRT4 antibodies (Abcam). The IHC results were independently examined by two pathologists blinded to patient data. Due to the heterogeneous intensity and distribution of reactivity across samples, immunostaining for SIRT4 was considered positive if $\geq 10\%$ of tumor cells were stained by the antibody in line with the criteria used in previous studies of other sirtuins (17). This study accessed gene expression data from the GEO database (<http://www.ncbi.nlm.nih.gov/geo/>), specifically datasets GSE33630 and GPL570, encompassing thyroid cancer and normal thyroid tissue samples. Raw data files were retrieved and preprocessed to ensure accuracy. The relationship between SIRT4 expression and thyroid cancer prognosis was investigated by Kaplan–Meier analysis using patient survival data and SIRT4 expression levels from TCGA data. SIRT4 expression was categorized as 'low' or 'high' based on the median expression value. Data processing and analysis were performed using GraphPad Prism (version 8.0; GraphPad Software, San Diego, CA, USA).

Cell culture and maintenance

Three human thyroid cancer cell lines, B-CPAP, TPC-1, and SNU-790, were used in this study. B-CPAP cell line was kindly provided by Soon-Hyun Ahn, MD, PhD (Seoul National University, Seoul, South Korea), and TPC-1 cell line (Sigma SCC147) was purchased from Sigma-Aldrich. SNU-790 cell line was obtained from the Korean Cell Line Bank (Seoul, South Korea). Cells were cultured in advanced RPMI 1640 medium (Thermo Fisher Scientific) supplemented with 10% v/v fetal bovine serum (FBS) sourced from GenDEPOT. The medium was further supplemented with 1% v/v penicillin/streptomycin and 200 mM L-glutamine, both from Thermo Fisher Scientific. Optimal cellular growth conditions were maintained at a temperature of 37°C in a 5% CO₂-enriched, humidified environment.

Generation of adenovirus expressing *SIRT4*

The ViralPower adenoviral expression system (Invitrogen by Thermo Fisher Scientific) was used to generate recombinant adenovirus harboring *SIRT4* (Ad-SIRT4). The cDNA corresponding to *SIRT4* was first cloned into the pENTR vector. After confirming the sequence integrity, the *SIRT4* cDNA was recombined into the pAd/CMV/V5-DEST gateway vector using LR Clonase II enzyme mix (Invitrogen). The resultant Ad-SIRT4 construct was linearized with PacI (New England Biolabs) and transfected into 293A cells using Lipofectamine 3000 (Invitrogen). Amplification of the generated viral particles in the same cell line was performed using the ViralPower adenoviral expression system (Invitrogen). Viral titers were determined using a plaque-forming assay with serial dilution. Thyroid cancer cell lines were exposed to aliquots of this viral suspension. Recombinant adenoviruses expressing green fluorescent protein (Ad-GFP) and β -galactosidase (Ad-LacZ) were used as controls.

Short hairpin RNA-mediated *SIRT4* silencing

SIRT4 knockdown was performed using bacterial glycerol stock harboring *SIRT4*-targeting short hairpin RNA (shRNA), RNA plasmid DNA (MISSION shRNA), and a non-targeting control plasmid (SHC002) obtained from Sigma-Aldrich. The silencing mechanism was powered by lentiviral delivery. Lentiviral particles were synthesized by co-transfecting *SIRT4*-targeting shRNA plasmids or non-targeting control shRNA plasmid with the MISSION Lentiviral Packaging Mix (SHP001; Sigma-Aldrich) into the 293FT cell line (Thermo Fisher Scientific) using Lipofectamine 3000 (Invitrogen). After transfection, cell culture supernatants enriched with lentiviral particles were collected at 24 and 48 h intervals. The supernatants were filtered and used to infect all thyroid cancer cell lines. Successful knockdown of *SIRT4* was determined by western blot analysis of whole-cell lysates.

Cell viability assessment with the Cell Counting Kit-8 assay

Cell viability was assessed using the Cell Counting Kit-8 (CCK-8, Tojindo, Kumamoto, Japan). Cells were seeded into 24-well plates at an optimal density. After a 24-h attachment period, cells were infected with Ad-GFP and Ad-SIRT6 adenoviruses or Lenti-shGFP and Lenti-shSirt4 lentiviruses. Cells were incubated for 72 h, and 50 μ L of CCK-8 solution were added to each well, followed by incubation for 2 h at 37°C in the dark. The optical density was measured at a wavelength of 450 nm using an ELISA reader.

Clonogenic survival assay

The colony-forming ability of cells was evaluated using a clonogenic assay. Cells were dissociated using

TrypLETM Express (Thermo Fisher Scientific) and quantified using an automatic cell counter. In total, 500 cells were seeded into each well of a 6-well plate. Following adherence, cells were infected with Ad-GFP and Ad-SIRT6 adenoviruses or Lenti-shGFP and Lenti-shSIRT4 lentiviruses. Plates were then placed in a humidified incubator at 37°C and 5% CO₂ and incubated for 10 or 14 days, and colonies were fixed and stained using a 0.5% crystal violet solution in methanol. Colonies consisting of more than 50 cells were counted manually.

Flow cytometric analysis of DNA content

Cell cycle distribution and apoptotic populations were determined by flow cytometry. The harvested cells were washed twice with ice-cold phosphate-buffered saline (PBS) and fixed by adding 70% ethanol dropwise while vortexing followed by incubation for 1 h at 4°C. The fixed cells were then treated with 1 mg/mL RNase A (Sigma-Aldrich) and stained with 50 μ g/mL PI (Sigma-Aldrich) for 30 min in the dark. The stained cells were analyzed on a Cytomics FC500 Flow Cytometer (Beckman-Coulter), and data were processed using CXP Software (Beckman-Coulter).

Measurement of mitochondrial ROS levels

The MitoSOX™ red mitochondrial superoxide indicator was used to monitor oxidative stress in cells. Cells at approximately 70–80% confluency were treated with 5 μ M MitoSOX reagent. Mitochondrial mass was assessed by incubating cells with 50 nM MitoTracker Deep Red for 30 min at 37°C in the dark. Following incubation, cells were detached using trypsin, washed with warm PBS, and resuspended in PBS. The fluorescence intensity, which indicates mitochondrial mass, was measured using a Cytomics FC500 Flow Cytometer (Beckman-Coulter). Quantification and median fluorescence intensity analyses were performed using CXP Software (Beckman-Coulter).

Flow cytometric analysis of apoptosis in human thyroid cancer cells

B-CPAP, TPC-1, and SNU-790 cells infected with Ad-GFP, Ad-SIRT4, Lenti-shGFP, and Lenti-shSIRT4 were subjected to apoptosis analysis using the Annexin V (FITC)-PI apoptosis detection kit (BD Biosciences) following the manufacturer's instructions. The cells were stained and processed for flow cytometry.

Transwell assays to assess cell invasion and migration

Cell invasion and migration were analyzed using Transwell plates (Costar, Cambridge, MA, USA) with 8 μ m-pore polycarbonate filters. For invasion-specific

assays, the upper chamber of the Transwell plates was pre-coated with BD Matrigel™ Basement Membrane Matrix (BD Biosciences, Bedford, MA, USA). Migration assays were performed without the Matrigel coating to assess the basic migratory properties without extracellular matrix penetration. Cell lines were prepared to a concentration of 1×10^5 cells/well and resuspended in advanced RPMI 1640 medium supplemented with 10% FBS. After 24 h of incubation at 37°C, cells that crossed the membrane by invasion or migration were immobilized with 4% paraformaldehyde and stained with 4',6-diamidino-2-phenylindole (DAPI) for visualization. Quantification was achieved using fluorescence microscopy in five arbitrarily selected fields at $\times 100$ magnification.

Gap closure assay for cell migration

For the gap closure assay, cells were seeded into an Ibidi Culture-Insert 2 well in a μ -dish 35 mm at a concentration of 1×10^5 cells/well using a serum-free medium. After 24 h, the culture-Insert 2 wWestern blot analysisell was carefully removed with sterile tweezers, and a standard culture medium was added. Time-lapse imaging of thyroid cancer cell lines was performed over 8 h, and images were captured every 2 h to monitor migration patterns.

Western blot analysis of protein expression

B-CPAP, TPC-1, and SNU-790 cells were lysed using radioimmunoprecipitation assay buffer (RIPA) lysis buffer (Thermo Fisher Scientific) supplemented with a protease inhibitor cocktail (GenDEPOT), sonicated for 2 min, and cell lysates were centrifuged at 14,000 *g* for 10 min at 4°C discarding insoluble fragments. Protein concentration was measured using a BCA protein assay kit (Pierce). Protein lysates (30 μ g of protein per lane) were resolved by SDS-PAGE and transferred onto nitrocellulose membranes (Millipore). Membranes were blocked with 5% BSA and then incubated with primary antibodies against E-cadherin, N-cadherin, MMP9, MMP3, SIRT4, SNAIL, and vimentin. After incubation with the corresponding horseradish peroxidase-conjugated secondary antibodies, protein bands were visualized with the Clarity Western blot ECL Substrate (Bio-Rad) and imaged with the ChemiDoc Touch Imaging System (Bio-Rad).

Immunohistochemical analysis of SIRT4 expression

Formalin-fixed, paraffin-embedded tissue sections from nude mice bearing B-CPAP tumors were processed for IHC examination. Tissue blocks were cut into 5 μ m-thick sections, which were de-paraffinized,

rehydrated, and incubated in 3% hydrogen peroxide for 10 min to inhibit endogenous peroxidase activity. Antigen retrieval was performed by heating the sections in 10 mM citrate buffer (pH 6.0) using a 700 W microwave oven for 20 min. For specific detection of SIRT4, the tissue sections were incubated with anti-SIRT4 antibodies (Abcam) overnight at 4°C.

Xenograft mouse model for *in vivo* assessment

All animal experiments were performed after obtaining approval from the Institutional Animal Care and Use Committee (IACUC) of Gyeongsang National University. All procedures strictly adhered to the stipulated National Research Council Guidelines. B-CPAP cell suspensions containing 5×10^6 cells per mouse were subcutaneously introduced into 6-week-old male athymic nude mice (procured from KOATECH corporation, Harlan, IN, USA). At 42 days post-cell inoculation, mice with xenograft tumors measuring 0.6–0.7 cm in diameter received intratumoral administrations of either Ad-GFP or Ad-SIRT4. Tumor dimensions were measured on days 42, 45, 48, and 54 using precision digital calipers, and the tumor volume was calculated using the modified ellipsoidal equation (tumor volume = $1/2(\text{length} \times \text{width}^2)$).

Analysis of apoptosis and oxidative stress in mouse tumors

Apoptosis and oxidative stress in mouse tumor tissues were evaluated in a terminal deoxynucleotidyl transferase (TdT)-mediated dUTP nick end labeling (TUNEL) assay and a dihydroethidium (DHE)-based assay. Briefly, samples were fixed overnight at room temperature in 4% formaldehyde, dehydrated in graded ethanol, permeated with xylene, and embedded in paraffin. Five-micrometer-thick sections were deparaffinized and treated for 10 min with 1% H₂O₂ (Cat. No. H1009, Sigma-Aldrich) to quench endogenous peroxidase. After rinsing in PBS (Cat. No. 10010023, Thermo Fisher Scientific), the sections were incubated for 6 min with 10 μ g/mL Proteinase K (Cat. No. EO0491, Thermo Fisher Scientific), followed for 6 min at 4°C in 0.1% Triton X-100 (Cat. No. T8787, Sigma-Aldrich). Subsequently, the slides were rinsed and incubated for 1 h at room temperature with 200 μ g/mL TdT mixture containing FITC-dUTP (Cat. No. BD556381, BD Biosciences, SJ, CA, USA). After rinsing with PBS, the sections were stained for 1 h with 10 μ mol/L DHE (Cat. No. D11347, Thermo Fisher Scientific) and then counterstained for 1 h with 0.5 μ g/mL DAPI (Cat. No. D9542, Sigma-Aldrich) solution. Analysis was performed using a research microscope equipped with Nikon software, and fluorescence intensity was quantified by measuring the percentage of positively stained areas in five random fields.

Statistical analysis

Statistical analysis was performed using SPSS software, version 20.0 (IBM), and GraphPad Prism (version 8.0; GraphPad Software). The relationship between *SIRT4* expression and clinicopathological parameters was assessed using the chi-square test, and differences between groups were analyzed using the Student's *t*-test. *P*-values <0.05 were considered significant.

Results

Role of *SIRT4* in GEO, TCGA database, and human PTC tissues

Analysis of data from the GEO database demonstrated that *SIRT4* is downregulated in thyroid cancer compared with normal thyroid tissues. In the TCGA database, overall survival was significantly better in patients with high *SIRT4* expression than in those with low *SIRT4* expression ($P=0.016$, Fig. 1A, B). The downregulation of *SIRT4* in thyroid cancer and its association with poor overall survival indicate that *SIRT4* may serve as a prognostic factor for thyroid cancer. Next, we evaluated *SIRT4* expression in PTC tissues. The demographic characteristics of the patients are shown in Supplementary 1 (see section on [supplementary materials](#) given at the end of this article). Clinical data showed that *SIRT4* expression varied among PTC tissue samples, which were divided into *SIRT4*-negative and *SIRT4*-positive groups according to *SIRT4* expression. Of 205 tissue samples, 86 were *SIRT4*-negative and 119 were *SIRT4*-positive (Fig. 1C). Comparison of patient clinical data according to the expression of *SIRT4* showed no statistically significant differences in

most parameters except for decreased extracapsular extension in *SIRT4*-positive patients ($P=0.000$) (Table 1). Taken together, these results suggest an association between *SIRT4* expression and the progression of thyroid cancer.

Effect of *SIRT4* expression on thyroid cancer cell proliferation

To further investigate the involvement of *SIRT4* in PTC, we evaluated its expression in three thyroid cancer cell lines. Western blot analysis of the baseline levels of sirtuins in B-CPAP cells showed that *SIRT1* had the highest expression, *SIRT5* had the lowest, and the other sirtuins including *SIRT4* had intermediate levels of expression (Fig. 2A). Next, we analyzed the effects of *SIRT4* overexpression and silencing in B-CPAP cells. The results of the CCK-8 assay showed that *SIRT4* overexpression decreased, whereas *SIRT4* knockdown increased cell viability significantly (Fig. 2B). In the clonogenic assay, *SIRT4* overexpression caused a significant reduction in the number of B-CPAP cell surviving clones, whereas *SIRT4* knockdown increased the number of clones compared with those in the control (Fig. 2C). The results of the CCK-8 and clonogenic assays for TPC-1 and SNU-790 cells were consistent, showing that *SIRT4* overexpression led to a decrease in cell viability and a reduction in the number of surviving clones (Supplementary 2).

Involvement of *SIRT4* in apoptosis and modulation of ROS levels

The percentage of sub-G1 cells increased gradually following the administration of Ad-*SIRT4* compared

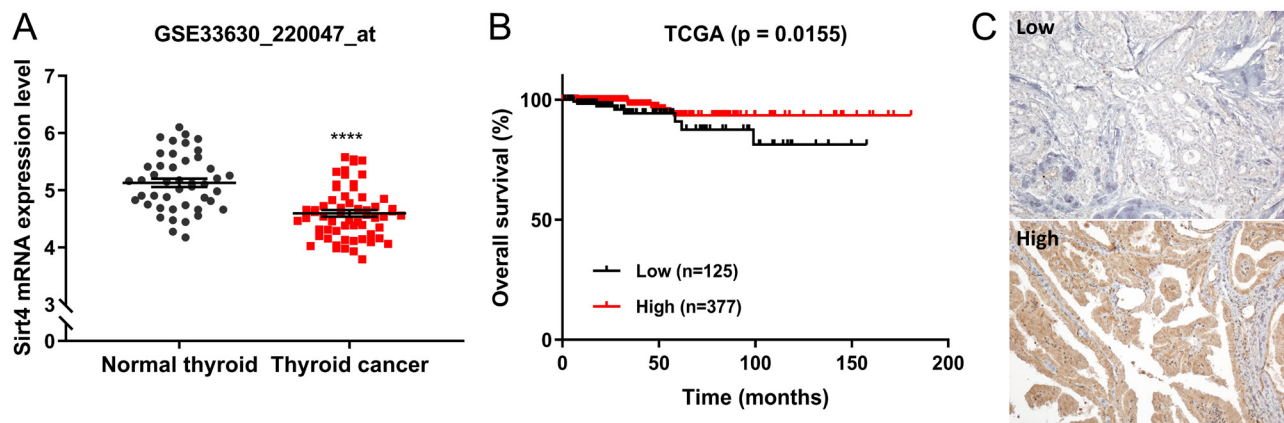


Figure 1

Clinical significance of *SIRT4* expression in thyroid cancer. (A) Analysis of the GSE33630 database showed that the mRNA expression levels of *SIRT4* are significantly lower in thyroid cancer tissues ($n = 45$) than in adjacent normal thyroid tissues ($n = 60$; $P < 0.0001$, *t*-test). (B) Overall survival was analyzed using a Kaplan-Meier (KM) plot based on the TCGA dataset, which included patients with high *SIRT4* expression and those with low *SIRT4* expression ($P = 0.0155$, log-rank test). (C) Representative IHC staining image of PTC tissues with different degrees of *SIRT4* expression. Number of positive cells: (-) <10%; (+) >10%. **** $P < 0.0001$. PTC, papillary thyroid carcinoma; TCGA, The Cancer Genome Atlas.

Table 1 Clinical characteristics of papillary thyroid carcinoma patients according to SIRT4 expression.

Variables	SIRT4 (-)	SIRT4 (+)	χ^2	P-value
Age (mean \pm s.d., years)	48.40 \pm 10.6	50.43 \pm 11.33	1.329	0.342
<55 years	59	74		
\geq 55 years	27	45		
Sex			0.881	0.718
Male	17	26		
Female	69	93		
ETE			0.334	0.000
(-)	40	86		
(+)	46	33		
LN metastasis			0.692	0.234
(-)	57	88		
(+)	29	31		
AJCC, 8th ed. stage			0.680	0.315
I	70	103		
II	16	16		

AJCC, American Joint Committee on Cancer; ETE, extrathyroid extension; LN, lymph node.

to the control cell line, reaching its highest level at 72 h. No significant differences in the sub-G1 population of B-CPAP cells were observed after *SIRT4* knockdown (Fig. 3A and B). *SIRT4* overexpression increased B-CPAP cell apoptosis compared with that in the control group, whereas *SIRT4* knockdown had no significant effect on the apoptosis rate (Fig. 3C and D). These findings suggest that *SIRT4* contributes to the regulation of the sub-G1 population in B-CPAP cells, and its overexpression may promote apoptosis.

The findings suggesting that *SIRT4* expression has an effect on apoptosis prompted us to investigate the

potential involvement of ROS. We found that *SIRT4* overexpression increased total ROS levels, whereas its downregulation decreased total ROS levels (Fig. 3E). To determine whether regulation of *SIRT4* modulates mitochondrial ROS levels, cells were stained with MitoSOX red. B-CPAP cells overexpressing *SIRT4* showed a marked increase in MitoSOX red fluorescence intensity over time compared with the control, indicating an increase in mitochondrial ROS levels. Overexpression of *SIRT4* substantially reduced MitoTracker Deep Red (MTDR) staining intensity compared with that in the control, indicating an association between reduced mitochondrial mass and apoptosis. Conversely, the downregulation of *SIRT4* decreased the intensity of MitoSOX red fluorescence and increased the intensity of MTDR (Fig. 3F). The experimental results for TPC-1 and SNU-790 cells also showed a similar trend (Supplementary 3), indicating that *SIRT4* overexpression increases mitochondrial ROS levels, thereby inducing apoptosis.

Effects of *SIRT4* on invasion, migration, and epithelial-mesenchymal transition-related protein expression

Next, we examined the effect of *SIRT4* on cell invasive and migratory abilities. *SIRT4* upregulation significantly decreased, whereas its downregulation increased invasion and migration compared with the control group (Fig. 4A–D). The results of the wound closure assay showed that the gap closure rate was significantly slower in cells overexpressing *SIRT4*, whereas it was accelerated following *SIRT4* knockdown (Fig. 4E and F). Collectively, these findings suggest that increased expression of *SIRT4* suppresses the invasive and migratory abilities of B-CPAP cells. To identify potential mechanisms underlying the

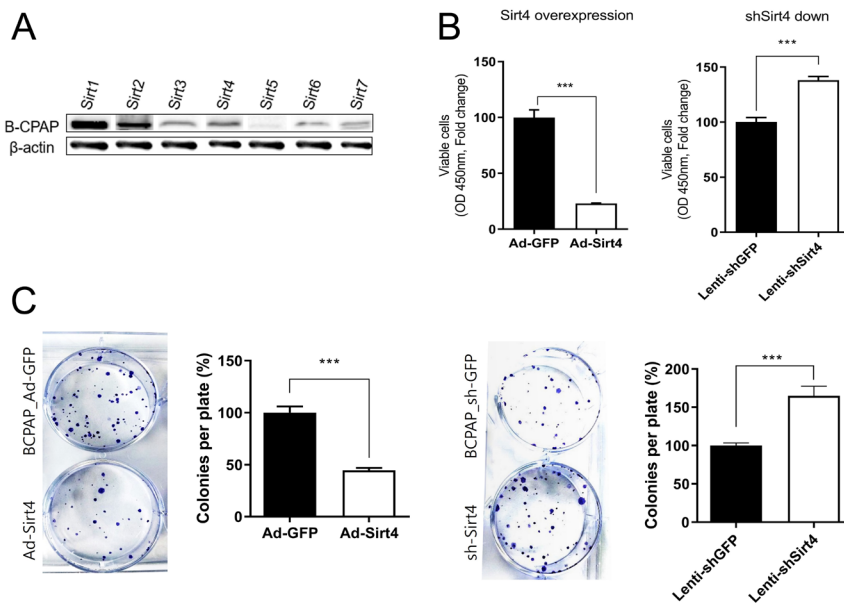


Figure 2

SIRT4 inhibits B-CPAP cell proliferation. (A) Western blot analysis of the expression levels of sirtuins in B-CPAP cells. (B) CCK-8 assay of *SIRT4*-overexpressing and sh*SIRT4*-transfected B-CPAP cells compared with the controls. B-CPAP cells were seeded into 24-well plates and treated with CCK-8 solution 72 h post seeding. *SIRT4* significantly suppressed the viability of B-CPAP cells. (C) Clonogenic assay of *SIRT4*-overexpressing and sh*SIRT4*-transfected B-CPAP cells compared with the controls. Surviving clones were decreased in *SIRT4*-overexpressing B-CPAP cells but increased in *SIRT4*-downregulated B-CPAP cells. * $P < 0.05$; ** $P < 0.01$; *** $P < 0.001$. CCK-8, Cell Counting Kit-8.

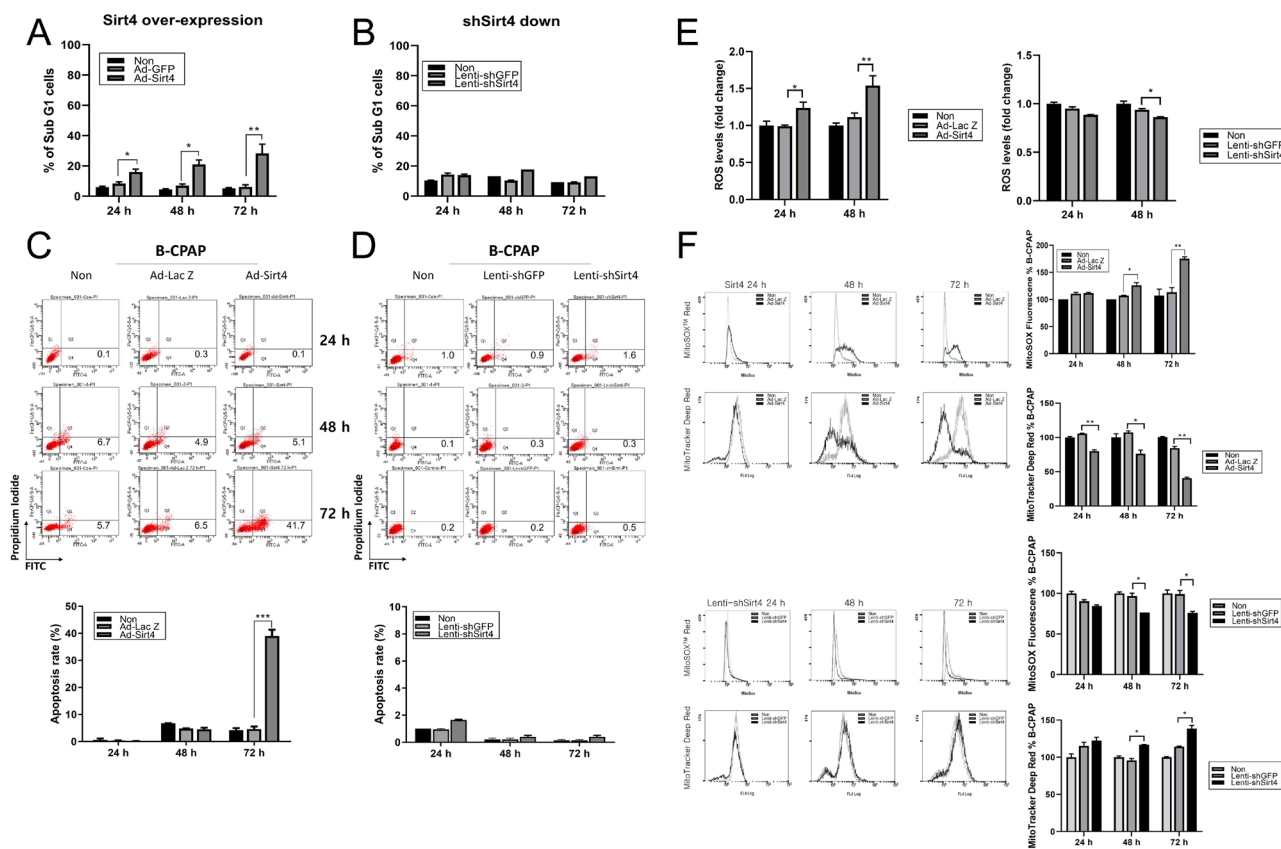


Figure 3

SIRT4 regulates the cell cycle and promotes cell death by modulating ROS levels in B-CPAP cells. (A) Percentage of cells in sub-G1 phase in control and *SIRT4*-overexpressing B-CPAP cells. B-CPAP cells were treated for 24, 48, and 72 h and examined by flow cytometry. Histograms represent PI fluorescence intensity. *SIRT4* overexpression significantly increased the number of sub-G1 cells. (B) Percentage of cells in sub-G1 phase in control and shSIRT4-transfected B-CPAP cells. (C) Apoptosis rate in control and *SIRT4*-overexpressing B-CPAP cells analyzed by flow cytometry using an Annexin V (FITC)-PI apoptosis detection kit. *SIRT4* overexpression significantly increased the apoptosis rate at 72 h. (D) Apoptosis rate in control and *SIRT4*-downregulated B-CPAP cells. (E) Differences in total ROS levels upon regulation of SIRT4 expression. (F) *SIRT4* upregulation significantly increased MitoSOX red levels and reduced the intensity of MTDR over time, and *SIRT4* downregulation had the opposite effect. MTDR, MitoTracker Deep Red; ROS, reactive oxygen species.

inhibitory effect of SIRT4, we examined the expression of epithelial-mesenchymal transition (EMT)-related proteins. *SIRT4* overexpression significantly upregulated the expression of E-cadherin and downregulated N-cadherin and other EMT markers. Downregulation of *SIRT4* decreased E-cadherin levels, and although it had no significant effect on N-cadherin expression, it upregulated other EMT markers such as MMP9 and vimentin (Fig. 4G). The cell invasion and migration assays for TPC-1 and SNU-790 cells also showed that *SIRT4* overexpression, as in B-CPAP cells, reduced their invasive and migratory abilities. In addition, we observed a consistent trend in the expression of EMT markers in all three human thyroid cancer cell lines (Supplementary 4).

Inhibition of tumor growth by SIRT4 in a B-CPAP xenograft mouse model

The present findings were confirmed *in vivo* in a xenograft mouse model generated by injecting B-CPAP

cells into mice, followed by intratumoral injection of Ad-GFP and Ad-SIRT4. Tumors were smaller in mice expressing *SIRT4* than in the control group (Fig. 5A). The volume and weight of excised tumors were significantly smaller in *SIRT4*-overexpressing mice compared to the control group, indicating that *SIRT4*-expressing B-CPAP cells delay tumor growth *in vivo* (Fig. 5B, C). Hematoxylin and eosin staining confirmed the presence of tumors established from B-CPAP cells, and IHC staining of tumor cells verified the expression of SIRT4 in tumors injected with Ad-SIRT4. The extent of apoptosis was evaluated by the TUNEL staining assay, which is a quantitative assay designed to ascertain the anti-tumor efficacy of SIRT4-induced apoptosis in PTC tumors. Expression of SIRT4 led to a four-fold increase in the number of TUNEL-positive apoptotic cells (with a high of 52.2% compared with 13% for control cells); cells were visualized as light green dots under a fluorescence microscope. DHE staining, used to monitor intratumoral production of ROS, revealed that ROS production in PTC increased

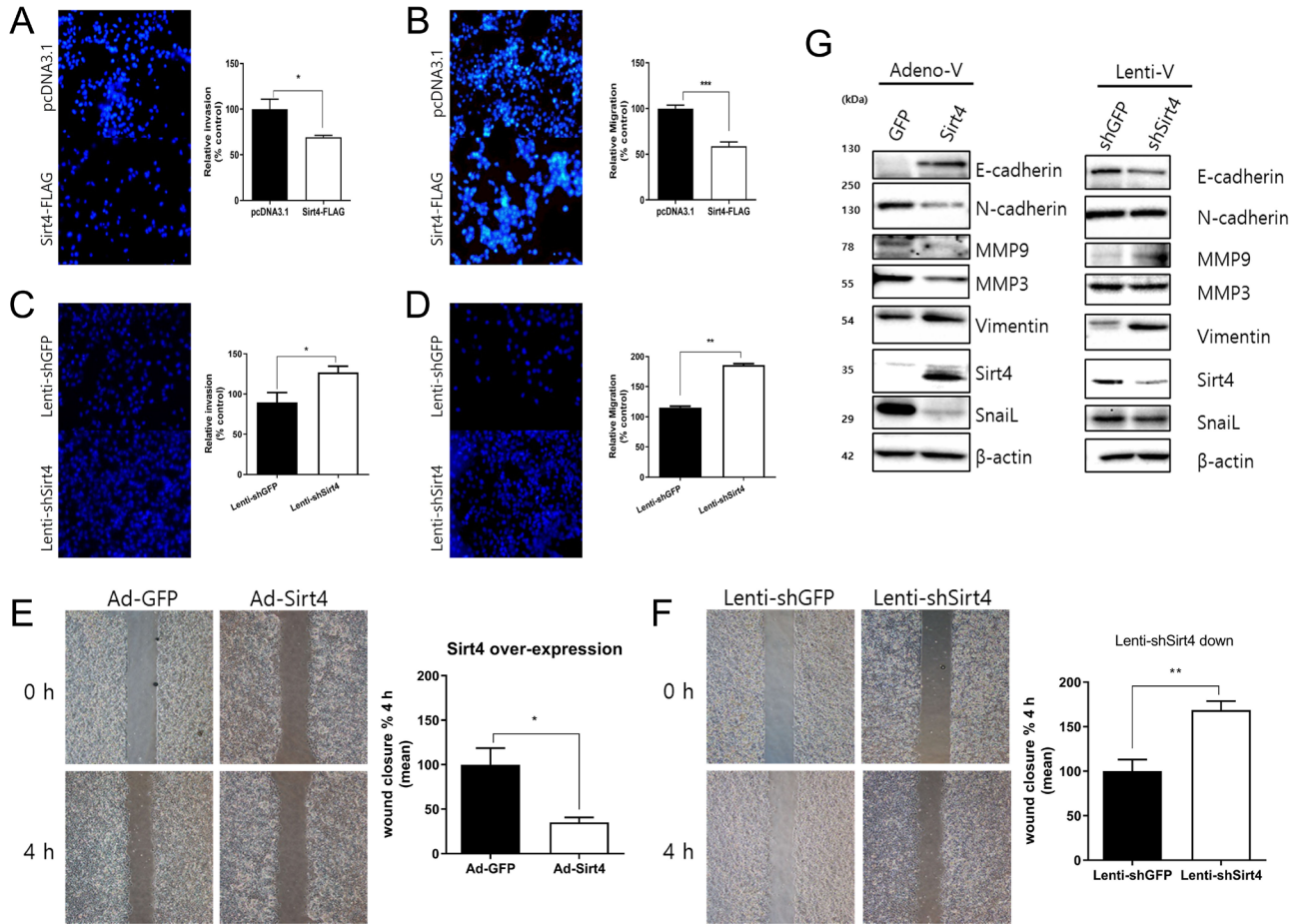


Figure 4

SIRT4 regulates the invasion and migration of B-CPAP cells by modulating the expression of EMT-related proteins. (A) Relative invasion and (B) migration abilities of *SIRT4*-overexpressing B-CPAP cells compared with the controls analyzed using Transwell assays. Cells were incubated for 24 h, and invaded and migrated cells were counted under a fluorescence microscope at $\times 100$ magnification in five random fields. (C) Relative invasion and (B) migration abilities of shSIRT4-transfected B-CPAP cells compared with the controls analyzed using Transwell assays. (E) Wound healing assays of SIRT4 overexpressing and (F) *SIRT4* knockdown cells compared with the controls. Representative images at the indicated times are on the right. (G) Modulation of EMT-related proteins by SIRT4 expression. The expression of E-cadherin, N-cadherin, and other EMT markers was analyzed and quantified. * $P < 0.05$, ** $P < 0.01$, *** $P < 0.001$. EMT, epithelial–mesenchymal transition.

markedly to 60.8% upon expression of SIRT4, compared with 15.8% in the controls, representing a 3.8-fold increase (Fig. 5D). Thus, the TUNEL and DHE staining results indicate that SIRT4 expression induces severe apoptotic stress in PTC by increasing ROS production. These findings provide further evidence to support the inhibitory effect of SIRT4 on B-CPAP cells.

Discussion

This study comprehensively examined the role of SIRT4 in the proliferation and progression of thyroid cancer, especially PTC, from multiple perspectives. First, we used data from the GEO and TCGA databases to examine the expression levels of SIRT4 in thyroid cancer and normal thyroid tissue and assessed the

impact of different SIRT4 expression levels on overall survival rates. We found that decreased SIRT4 expression in thyroid cancer samples was associated with lower overall survival rates. Analysis of clinical and pathological data from PTC tissue specimens showed that SIRT4 expression is negatively correlated with extracapsular extension in PTC, indicating a potential tumor suppressor function for SIRT4 in PTC. *In vitro* experiments using B-CPAP, TPC-1, and SNU-790 cells showed that SIRT4 overexpression decreased cell viability, promoted apoptosis, and suppressed colony formation, and *SIRT4* knockdown had the opposite effects. Increased SIRT4 levels suppressed the migration and invasion of B-CPAP, TPC-1, and SNU-790 cells, whereas decreased SIRT4 expression had the opposite effect. The data indicate that SIRT4 might inhibit thyroid cancer cell growth and survival

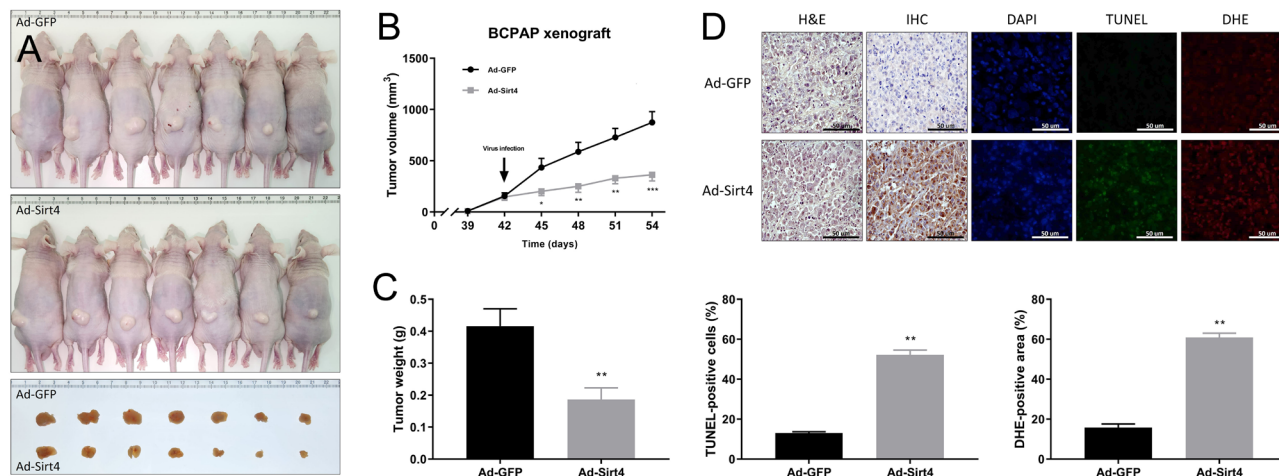


Figure 5

SIRT4 inhibits tumor growth in a B-CPAP xenograft mouse model. (A) On day 42 after implanting tumor cells, mice received intratumoral injections of Ad-GFP or Ad-SIRT4. The tumor images show excised tumors from each group, with the top group representing the control group and the bottom group representing the SIRT4-expression group. (B) Tumor diameter was measured every 3 days using digital calipers and tumor volume was calculated. The diagram shows the tumor growth curve of the 14 mice at the indicated times after intratumoral injections of Ad-GFP or Ad-SIRT4. (C) Tumor weight was compared between the SIRT4-expression group and the control group. (D) *SIRT4* overexpression induces apoptosis and superoxide production in mouse tumors. FFPE sections of tumors were co-stained with DAPI (0.5 µg/mL) to visualize nuclei, along with TdT enzyme (200 µg/mL) and DHE (10 µmol/L) to detect apoptosis and superoxide production, respectively. Apoptotic green fluorescence, oxidative red fluorescence, and nuclear blue fluorescence were analyzed under a fluorescence microscope at 400× magnification. The graph below shows the quantified signal of cells stained positively by TdT and DHE in five random fields. *n* = 8. **P* < 0.05, ***P* < 0.01, ****P* < 0.001. DAPI, 4',6-diamidino-2-phenylindole; DHE, dihydroethidium; FFPE, formalin-fixed paraffin-embedded; TdT, terminal deoxynucleotidyl transferase; TUNEL, TdT-mediated dUTP nick end labeling.

and affect the metastatic potential. The tumor-suppressive role of SIRT4 in thyroid cancer was verified in an *in vivo* xenograft mouse model.

Overall, the present findings suggest that SIRT4 plays a tumor-suppressive role in thyroid cancer by impeding cell growth, survival, and metastasis. These findings are consistent with previous studies demonstrating the tumor-suppressive capacity of SIRT4 in various malignancies such as breast cancer, colorectal cancer, prostate cancer, and hepatocellular carcinoma (18, 19, 20, 21). A comprehensive meta-analysis of *SIRT4* expression in human tumors showed that *SIRT4* mRNA is downregulated in several malignant carcinomas compared with their normal counterparts (14). Several factors could be involved in the inhibitory effect of SIRT4 on thyroid cancer. SIRT4 regulates the inflammatory response and oxidative stress, and SIRT4 downregulation decreases ROS levels (22, 23). In this study, SIRT4 overexpression decreased the mitochondrial membrane potential and increased ROS levels, suggesting that the inhibitory effect of SIRT4 could be related to the regulation of mitochondrial function and oxidative stress in thyroid cancer. Invasiveness is a major determinant of the prognosis of various cancers. We analyzed the expression of EMT-related proteins to elucidate the potential mechanisms underlying the impact of SIRT4 on invasion and migration capabilities. Increased SIRT4 levels upregulated the expression of the epithelial marker E-cadherin and downregulated the mesenchymal

marker N-cadherin and other EMT-related proteins including MMP9, MMP3, and SNAIL. Decreased SIRT4 levels showed the opposite effect. This modulation of EMT-related proteins might affect the invasive potential of cancer. Loss of E-cadherin disrupts intercellular contacts and increases the motility and invasiveness of cells, promoting EMT in cancer cells (24, 25). Miyo *et al.* reported that SIRT4 inhibits EMT by decreasing

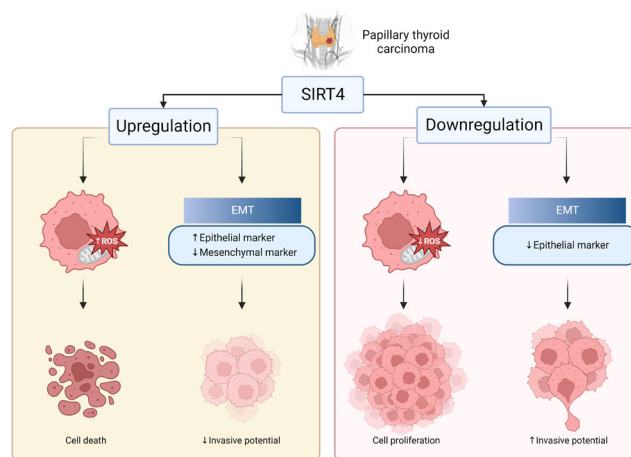


Figure 6

Schematic diagram of the role of SIRT4 on papillary thyroid cancer cells. Figure created with BioRender.com.

the levels of intracellular dimethyl- α -ketoglutarate through the inhibition of glutamate dehydrogenase in human colorectal cancer (26). Collectively, these findings indicate that SIRT4 may play a crucial role in regulating tumor growth and the invasive potential of thyroid cancer through the modulation of ROS levels and the expression of EMT-related proteins (Fig. 6).

The present study had several limitations. First, the sample size of PTC tissues used for the clinical data analysis was relatively small, which may limit the generalizability of the results. To validate the findings and ensure robustness, further large-scale studies are needed for cross-validation with clinical data. Second, we used tissue microarrays to examine a large number of tissues simultaneously, which limited our ability to assess the peri-tumor microenvironment. Moreover, the findings are limited to differences in the SIRT4 expression by thyroid cancer cells; therefore, further evaluation of differences between thyroid cancer cells and normal thyroid cells is required to confirm the potential of SIRT4 as a therapeutic target. Lastly, although we investigated the potential factors responsible for the effect of SIRT4, the precise molecular mechanisms underlying these effects are not fully understood. Proposed mechanisms include regulation of glutamine metabolism and genomic instability and regulation of the p53 signaling pathway. SIRT4 inhibits the enzymatic activity of glutamine dehydrogenase, thereby reducing glutamine anaplerosis and supporting cell survival under conditions of DNA damage (27). Moreover, treatment with dimethyl α -ketoglutarate increases wound healing and invasiveness significantly, suggesting that SIRT4 suppresses migration and invasion of B-CPAP cells by inhibiting glutamine metabolism (28). Li *et al.* reported that SIRT4 promotes phosphorylation of p53, which in turn induces cellular autophagy. These results indicate that SIRT4 inhibits tumorigenesis by upregulating the p53 signaling pathway (29). Future studies should focus on identifying the signaling pathways and molecular interactions mediating the tumor-suppressive effects of SIRT4.

In conclusion, this study provides novel insight into the potential contribution of SIRT4 in regulating the pathological progression of PTC. Our results suggest that SIRT4 plays a crucial tumor-suppressive role in PTC by inhibiting cell growth, survival, and invasive potential. Further research is necessary to validate these findings and to explore the detailed molecular mechanisms underlying the effect of SIRT4 in PTC and normal thyroid tissue; data from such studies will provide fundamental information that may contribute to the development of new therapeutic strategies for PTC.

Supplementary materials

This is linked to the online version of the paper at <https://doi.org/10.1530/ETJ-24-0079>.

Declaration of interest

The authors declare that they have no known competing financial interests or personal relationships that could have appeared to influence the work reported in this paper.

Funding

This work has been supported by a National Research Foundation of Korea (NRF) grant funded by the Korean government (NRF-2021R1F1A1056420, NRF-2022R1F1A10750), Institute of Health Sciences of Gyeongsang National University (IHS GNU-2022-05), and the Biomedical Research Institute fund (GNUHBRIF-2024-0004) of Gyeongsang National University Hospital.

Author contribution statement

Conceptualization: JJP, HJL, YSH, JHS; Methodology: JJP, YSH, JHS; Validation: JJP, HJL, YSH; Formal analysis: JJP, HJL, YSH, SYC, SJW, SJL; Funding acquisition: SJW; Investigation: HJL, YSH, SYC, SR, JHS; Resources: SYC, SJW, CDY, SJL; Data Curation: SYC, SJW, CDY, SJL; Writing – Original Draft: HJL, SYC, SJL; Writing – Review and Editing: JJP, HJL, YSH, SR, JHS; Visualization: CDY, SR, SJL, JHS; Supervision: JJP, YSH, SJW; Project administration: JJP, HJL, YSH.

Acknowledgement

The authors gratefully acknowledge the invaluable assistance of Soon-Hyun Ahn, MD, PhD (Seoul National University).

References

- Agate L, Lorusso L & Elisei R. New and old knowledge on differentiated thyroid cancer epidemiology and risk factors. *Journal of Endocrinological Investigation* 2012 **35**(Supplement) 3–9.
- Hundahl SA, Fleming ID, Fremgen AM & Menck HR. A national cancer data base report on 53,856 cases of thyroid carcinoma treated in the U.S., 1985–1995 (see comments). *Cancer* 1998 **83** 2638–2648. ([https://doi.org/10.1002/\(sici\)1097-0142\(19981215\)83:12<2638::aid-cnrc31>3.0.co;2-1](https://doi.org/10.1002/(sici)1097-0142(19981215)83:12<2638::aid-cnrc31>3.0.co;2-1))
- Chen D, Tan Y, Li Z, Li W, Yu L, Chen W, Liu Y, Liu L, Guo L, Huang W, *et al.* Organoid cultures derived from patients with papillary thyroid cancer. *Journal of Clinical Endocrinology and Metabolism* 2021 **106** 1410–1426. (<https://doi.org/10.1210/clinem/dgab020>)
- Toniato A, Boschin I, Casara D, Mazzarotto R, Rubello D & Pelizzo M. Papillary thyroid carcinoma: factors influencing recurrence and survival. *Annals of Surgical Oncology* 2008 **15** 1518–1522. (<https://doi.org/10.1245/s10434-008-9859-4>)
- Ito Y, Kudo T, Kobayashi K, Miya A, Ichihara K & Miyauchi A. Prognostic factors for recurrence of papillary thyroid carcinoma in the lymph nodes, lung, and bone: analysis of 5,768 patients with average 10-year follow-up. *World Journal of Surgery* 2012 **36** 1274–1278. (<https://doi.org/10.1007/s00268-012-1423-5>)
- Chen J, Wang D, Xu R, Yao T, Guo Y, Liu Q, Yang E, Wu Z & Xu Z. SLP-2 regulates the generation of reactive oxygen species and the ERK pathway to promote papillary thyroid carcinoma motility and angiogenesis. *Tissue and Cell* 2023 **80** 101997. (<https://doi.org/10.1016/j.tice.2022.101997>)
- Ha HC, Thiagalingam A, Nelkin BD & Casero RA, Jr. Reactive oxygen species are critical for the growth and differentiation of medullary thyroid carcinoma cells. *Clinical Cancer Research* 2000 **6** 3783–3787.
- Abooshahab R, Hooshmand K, Razavi F, Dass CR & Hedayati M. A glance at the actual role of glutamine metabolism in thyroid

- tumorigenesis. *Excli Journal* 2021 **20** 1170–1183. (<https://doi.org/10.17179/excli2021-3826>)
- 9 Zhang GQ, Xi C, Ju NT, Shen CT, Qiu ZL, Song HJ & Luo QY. Targeting glutamine metabolism exhibits anti-tumor effects in thyroid cancer. *Journal of Endocrinological Investigation* 2024 **47** 1953–1969. (<https://doi.org/10.1007/s40618-023-02294-y>)
 - 10 Kupis W, Pałyga J, Tomal E & Niewiadomska E. The role of sirtuins in cellular homeostasis. *Journal of Physiology and Biochemistry* 2016 **72** 371–380. (<https://doi.org/10.1007/s13105-016-0492-6>)
 - 11 Tomaselli D, Steegborn C, Mai A & Rotili D. Sirt4: a multifaceted enzyme at the crossroads of mitochondrial metabolism and cancer. *Frontiers in Oncology* 2020 **10** 474. (<https://doi.org/10.3389/fonc.2020.00474>)
 - 12 Jeong SM, Hwang S & Seong RH. SIRT4 regulates cancer cell survival and growth after stress. *Biochemical and Biophysical Research Communications* 2016 **470** 251–256. (<https://doi.org/10.1016/j.bbrc.2016.01.078>)
 - 13 Wang C, Liu Y, Zhu Y & Kong C. Functions of mammalian SIRT4 in cellular metabolism and research progress in human cancer. *Oncology Letters* 2020 **20** 11. (<https://doi.org/10.3892/ol.2020.11872>)
 - 14 Bai Y, Yang J, Cui Y, Yao Y, Wu F, Liu C, Fan X & Zhang Y. Research progress of Sirtuin4 in cancer. *Frontiers in Oncology* 2020 **10** 562950. (<https://doi.org/10.3389/fonc.2020.562950>)
 - 15 Csibi A, Fendt SM, Li C, Poulogiannis G, Choo AY, Chapski DJ, Jeong SM, Dempsey JM, Parkhitko A, Morrison T, *et al.* The mTORC1 pathway stimulates glutamine metabolism and cell proliferation by repressing SIRT4. *Cell* 2013 **153** 840–854. (<https://doi.org/10.1016/j.cell.2013.04.023>)
 - 16 Huang G, Lin Y & Zhu G. SIRT4 is upregulated in breast cancer and promotes the proliferation, migration and invasion of breast cancer cells. *International Journal of Clinical and Experimental Pathology* 2017 **10** 11849–11856.
 - 17 Lv L, Shen Z, Zhang J, Zhang H, Dong J, Yan Y, Liu F, Jiang K, Ye Y & Wang S. Clinicopathological significance of SIRT1 expression in colorectal adenocarcinoma. *Medical Oncology* 2014 **31** 965. (<https://doi.org/10.1007/s12032-014-0965-9>)
 - 18 Shi Q, Liu T, Zhang X, Geng J, He X, Nu M & Pang D. Decreased sirtuin 4 expression is associated with poor prognosis in patients with invasive breast cancer. *Oncology Letters* 2016 **12** 2606–2612. (<https://doi.org/10.3892/ol.2016.5021>)
 - 19 Huang G, Cheng J, Yu F, Liu X, Yuan C, Liu C, Chen X & Peng Z. Clinical and therapeutic significance of sirtuin-4 expression in colorectal cancer. *Oncology Reports* 2016 **35** 2801–2810. (<https://doi.org/10.3892/or.2016.4685>)
 - 20 Mao L, Hong X, Xu L, Wang X, Liu J, Wang H, Qian Y, Zhao J & Jia R. Sirtuin 4 inhibits prostate cancer progression and metastasis by modulating p21 nuclear translocation and glutamate dehydrogenase 1 ADP-ribosylation. *Journal of Oncology* 2022 **2022** 5498743. (<https://doi.org/10.1155/2022/5498743>)
 - 21 Huang FY, Wong DK, Seto WK, Mak LY, Cheung TT & Yuen MF. Tumor suppressive role of mitochondrial sirtuin 4 in induction of G2/M cell cycle arrest and apoptosis in hepatitis B virus-related hepatocellular carcinoma. *Cell Death Discovery* 2021 **7** 88. (<https://doi.org/10.1038/s41420-021-00470-8>)
 - 22 Dai Y, Liu S, Li J, Li J, Lan Y, Nie H & Zuo Y. SIRT4 suppresses the inflammatory response and oxidative stress in osteoarthritis. *American Journal of Translational Research* 2020 **12** 1965–1975.
 - 23 Han Y, Zhou S, Coetzee S & Chen A. SIRT4 and its roles in energy and redox metabolism in health, disease and during exercise. *Frontiers in Physiology* 2019 **10** 1006. (<https://doi.org/10.3389/fphys.2019.01006>)
 - 24 Wu Y & Zhou BP. New insights of epithelial-mesenchymal transition in cancer metastasis. *Acta Biochimica et Biophysica Sinica* 2008 **40** 643–650. (<https://doi.org/10.1111/j.1745-7270.2008.00443.x>)
 - 25 Huang Y, Hong W & Wei X. The molecular mechanisms and therapeutic strategies of EMT in tumor progression and metastasis. *Journal of Hematology and Oncology* 2022 **15** 129. (<https://doi.org/10.1186/s13045-022-01347-8>)
 - 26 Miyo M, Yamamoto H, Konno M, Colvin H, Nishida N, Koseki J, Kawamoto K, Ogawa H, Hamabe A, Uemura M, *et al.* Tumour-suppressive function of SIRT4 in human colorectal cancer. *British Journal of Cancer* 2015 **113** 492–499. (<https://doi.org/10.1038/bjc.2015.226>)
 - 27 Jeong SM, Xiao C, Finley LW, Lahusen T, Souza AL, Pierce K, Li YH, Wang X, Laurent G, German NJ, *et al.* SIRT4 has tumor-suppressive activity and regulates the cellular metabolic response to DNA damage by inhibiting mitochondrial glutamine metabolism. *Cancer Cell* 2013 **23** 450–463. (<https://doi.org/10.1016/j.ccr.2013.02.024>)
 - 28 Chen Z, Lin J, Feng S, Chen X, Huang H, Wang C, Yu Y, He Y, Han S, Zheng L, *et al.* SIRT4 inhibits the proliferation, migration, and invasion abilities of thyroid cancer cells by inhibiting glutamine metabolism. *Oncotargets and Therapy* 2019 **12** 2397–2408. (<https://doi.org/10.2147/OTT.S189536>)
 - 29 Li J, Zhan H, Ren Y, Feng M, Wang Q, Jiao Q, Wang Y, Liu X, Zhang S, Du L, *et al.* Sirtuin 4 activates autophagy and inhibits tumorigenesis by upregulating the p53 signaling pathway. *Cell Death and Differentiation* 2023 **30** 313–326. (<https://doi.org/10.1038/s41418-022-01063-3>)